Supporting Information

Vatakis et al. 10.1073/pnas.1115050108

SI Methods

Isolation and Transduction of CD34 Human Hematopoietic Stem Cells. Fresh human fetal liver was obtained from Advanced Bioscience Resources, Inc. The tissue was homogenized and digested with collagenase, DNase, and hyaluronidase in Iscove's Modified Dulbecco's Medium. Cells were purified by Ficoll and cultured overnight at 37 °C, 5% CO_2 in RPMI 1640 supplemented by 10% (vol/vol) FCS and 0.44 mg/mL pip/tazo (piperacillin and tazobactam) (Sigma-Aldrich) at a concentration of 10^6 cells/mL Subsequently, CD34 cells were sorted using the direct human CD34 kit (Miltenyi Biotech) on an AutoMACS cell sorter (Miltenyi). Fresh CD34 cells were resuspended in 2% (vol/vol) human serum albumin containing Yssel's medium and placed into a six-well plate coated with 20 mg/mL retronectin (Takara Bio, Inc.) with the lentiviral vector at a multiplicity of infection of 5 overnight at 37 °C. Cells then were washed, placed in plain Eagle's minimal essential medium (MEM), and used for the generation of the marrow/liver/thymus (BLT) mice. A fraction of the transduced cells was frozen to be used in CD34 cell injections.

Cytotoxic T Lymphocyte Killing Assay. The M202 and M207 targets (10^6 cells/mL) were labeled with a green fluorescent membrane dye, $DiOC_{18}$, in PBS at 37 °C according to the manufacturer's recommendations. Subsequently, cells were washed with medium and mixed with effector splenocytes at different effector:target ratios. Then, propidium iodide (PI) was added to the mixed cells to measure cell death of the compromised target cells. Cell cytotoxicity is measured as a percentage of $DiOC_{18}{}^{+}PI^{+}$ cells. Effectors and targets were incubated for 4 h at 37 °C followed by flow cytometric analysis using a Coulter FC500 instrument and FlowJo software (TreeStar, Inc.).

PET and CT Imaging. Mice were fasted for 4–6 h before [^{18}F]-fluorodeoxyglucose ([^{18}F]FDG) injection and were placed on a heating pad (30 °C) 30 min before [^{18}F]FDG injection. For tracer injection and imaging, mice were anesthetized with 2% isoflurane. Mice were imaged in a chamber that minimizes positioning errors between PET and CT to <1 mm. Imaging started 60 min after an i.p. injection of 7.4 MBq (80 μCi) [^{18}F]FDG or [^{18}F]-fluoro-3hydroxymethylbutyl)guanine ([^{18}F]HBG) via tail vein. Image acquisition time was 10 min. Images were reconstructed using a combination of 3D-ordered subset-expectation maximization (SOEM3D) and Maximus A Priori (MAP). The number of OSEM subsets used was 16. The number of MAP iterations used was 18. Image counts per pixel per second were calibrated to activity concentrations (Bq/mL) by measuring a 3-cm cylinder phantom filled with a known concentration of [^{18}F]FDG. Immediately after the PET scan, the mice underwent an 8-min microCT scan using routine image acquisition variables (70 kVP and 500 μA). For display, activity concentrations were expressed as percent of the decay-corrected injected activity per gram of tissue by using OsiriX (Pixmeo) software. Spherical regions of interest (2-mm diameter) were placed in the area of the tumor with the highest [^{18}F]FDG or [^{18}F]HBG uptake. All image analysis was done using the OsiriX software.

Real-Time PCR Analysis. Because the lentiviral vector used in these studies was HIV based, we used an HIV-based quantitative real-time DNA PCR to detect the presence of vector in CD34 cells. The assays was performed using a primer/probe pair that amplifies cellular β-globin sequences: forward (BGF1) 5′-CAACCTCAAACAGACACCATG-3′; reverse (BGR1) 5′-TCCAGTTCACCTTGCCC-3′; probe (BGX1) 6FAM 5′-CTCCTGAGGAGAAGTCTGCCGTTACTGCC-3′) and a primer/probe pair that amplifies full-length HIV reverse transcripts (LTR/gag junction): SR1 5′-CAAGTAGTGTGTGCCCGTCTGT-3′; 661 5′-CCTGCGTCGAGAG AGCTCCTCTGG-3′; probe ZXF 6FAM 5′-TGTGACTCTGGTAACTAGAGATC CCTCAGACCC-3′). All amplifications were performed in parallel with a set of known quantitative standards. The standard curve to determine HIV DNA levels ranges from 10–20,000 copies of cloned HIV DNA. The standard curve to determine levels of β-globin gene sequences consists of DNA derived from 10–100,000 normal human peripheral blood lymphocytes. Quantitation of HIV-1 sequences was achieved by extrapolation from these standard curves.

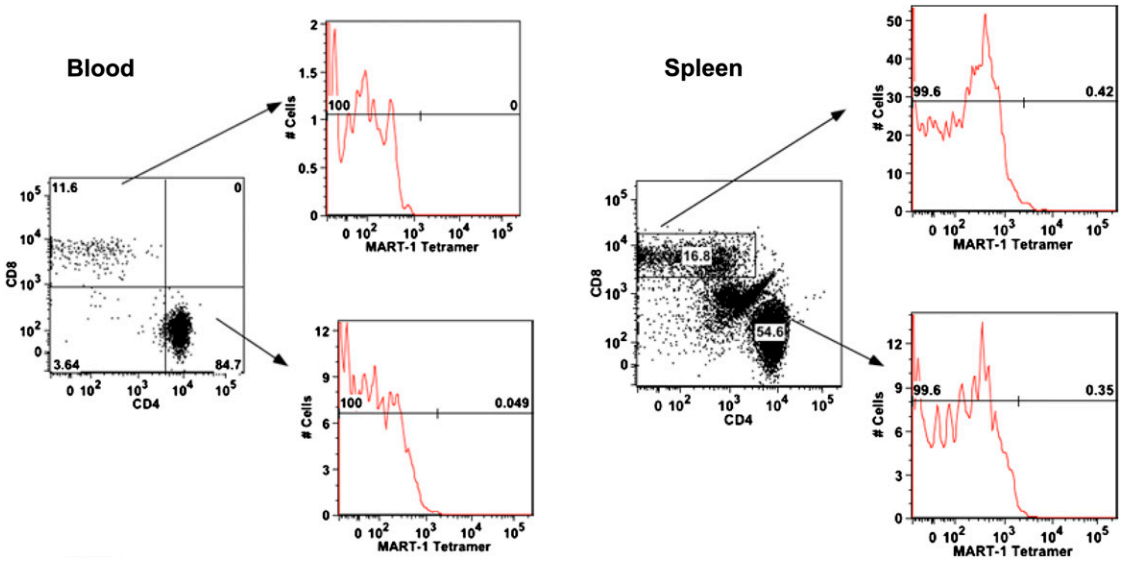

Fig. S1. Melanoma-associated antigen recognized by T-cells 1 (MART-1)–transgenic CD8 T cells are selected in the thymus/liver implant. A series of BLT mice were generated using an HLA-A*0201^{-} fetal liver and thymus. The data presented in this figure show one representative mouse (of five). The blood and spleen samples were collected at the end point of the experiment and were stained for CD3, CD4, CD8, CD45, and MART-1 tetramer. Samples were gated on CD45^{+} and CD3^{+} cells to exclude murine and non–T-cell populations. We did not observe any circulating MART-1^{+} T cells.

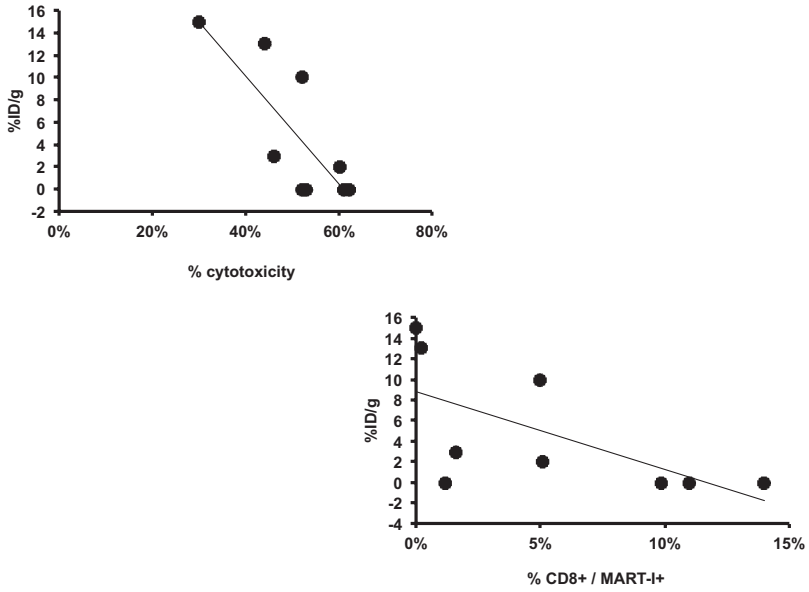

Fig. S2. Correlation of tumor clearance with transgenic T-cell reconstitution and killing activity. Based on the data in Table S1, we generated correlation analyses from our second cohort of mice. In both sets of data, the correlation is statistically significant ($P < 0.05$) based on a Spearman correlation test. %ID/g, injected dose per gram of body weight.

Table S1. Cumulative data from the second mouse cohort used in correlation of tumor clearance with MART-1–specific T-cell reconstitution and cytolytic activity

Mouse ID	% $CD8^+Tetramer^+$	CTL killing (%)	202 Tumor (%ID/G)
6	1	61	0
7	0	44	13
8	6	52	10
9	10	52	0
10	2	46	3
16	14	62	0
18	11	53	0
19	*5*	*60*	*2*
20	0	30	15

The correlation tests shown in Fig. S1 were based on the results displayed in this table. Mouse 6 deviated from the trend observed in mice with high levels of $CD8^+$tetramer$^+$ cells. In this mouse, we detected high levels of tetramer$^+$ cells (12.8% of $CD45^+CD8^+$MART-1^+ cells) in the M202 tumor. CTL, cytotoxic T lymphocyte; %ID/g, injected dose per gram of body weight.

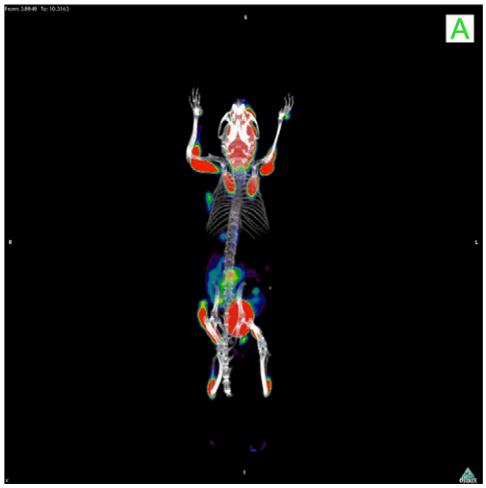

Movie S1. Reconstructed tridimensional PET CT scan. BLT mice injected with M202 (*Left*) and M207 (*Right*) tumors and scanned at the end point of the experiments with [^{18}F]FDG tracer injection. The upper right cube indicates mouse orientation: A, anterior; P, posterior, L, left; R, right. In addition, the left and right side of the mouse are indicated as *L* and *R* on the left and right sides of the animation.

Movie S1

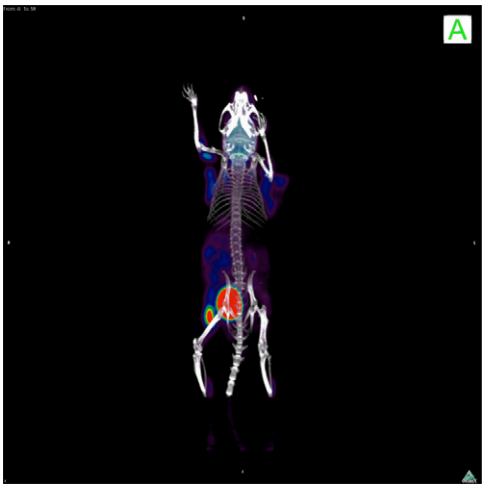

Movie S2. Reconstructed tridimensional PET CT scan. BLT mice injected with M202 (*Left*) and M207 (*Right*) tumors and scanned at the end point of the experiments with [^{18}F]FDG tracer injection. The upper right cube indicates mouse orientation: A, anterior; P, posterior, L, left; R, right. In addition, the left and right side of the mouse are indicated as *L* and *R* on the left and right sides of the animation.

Movie S2

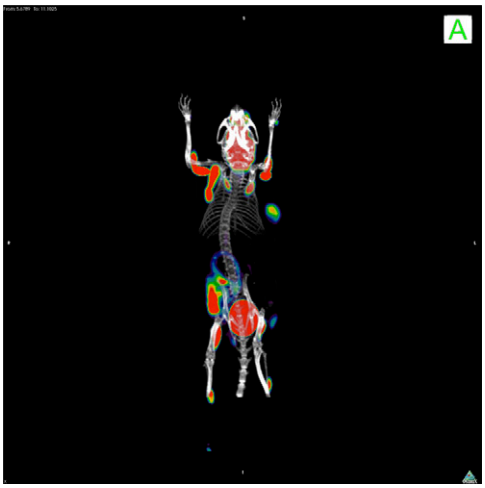

Movie S3. Reconstructed tridimensional PET CT scan. BLT mice injected with M202 (*Left*) and M207 (*Right*) tumors and scanned at the end point of the experiments with [^{18}F]FDG tracer injection. The upper right cube indicates mouse orientation: A, anterior; P, posterior, L, left; R, right. In addition, the left and right side of the mouse are indicated as *L* and *R* on the left and right sides of the animation.

Movie S3

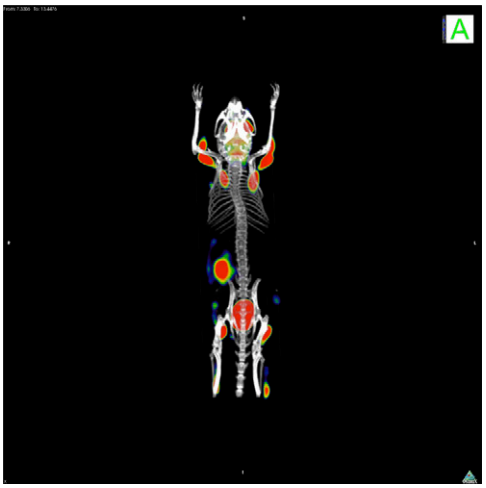

Movie S4. Reconstructed tridimensional PET CT scan. BLT mice injected with M202 (*Left*) and M207 (*Right*) tumors and scanned at the end point of the experiments with [^{18}F]FDG tracer injection. The upper right cube indicates mouse orientation: A, anterior; P, posterior, L, left; R, right. In addition, the left and right side of the mouse are indicated as *L* and *R* on the left and right sides of the animation.

Movie S4

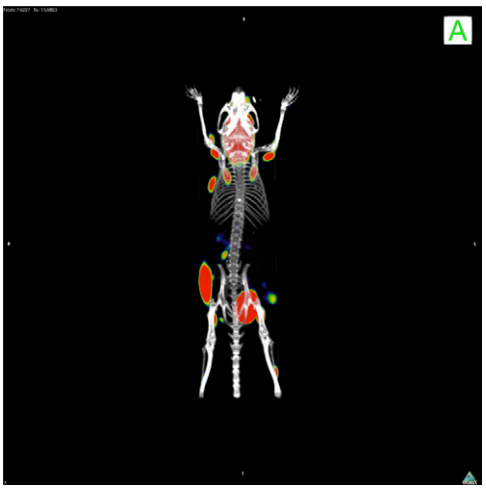

Movie S5. Reconstructed tridimensional PET CT scan. BLT mice injected with M202 (*Left*) and M207 (*Right*) tumors and scanned at the end point of the experiments with [^{18}F]FDG tracer injection. The upper right cube indicates mouse orientation: A, anterior; P, posterior, L, left; R, right. In addition, the left and right side of the mouse are indicated as *L* and *R* on the left and right sides of the animation.

Movie S5

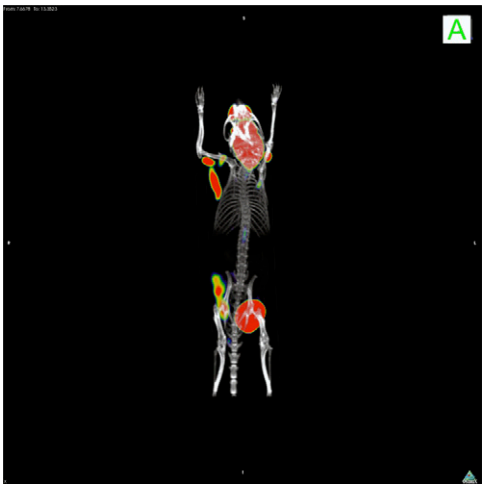

Movie S6. Reconstructed tridimensional PET CT scan. BLT mice injected with M202 (*Left*) and M207 (*Right*) tumors and scanned at the end point of the experiments with [^{18}F]FDG tracer injection. The upper right cube indicates mouse orientation: A, anterior; P, posterior, L, left; R, right. In addition, the left and right side of the mouse are indicated as *L* and *R* on the left and right sides of the animation.

Movie S6

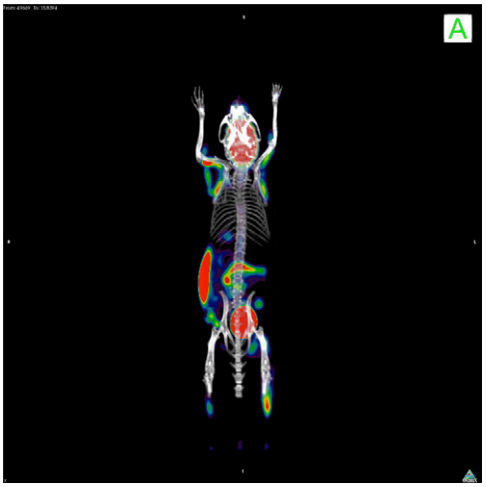

Movie S7. Reconstructed tridimensional PET CT scan. BLT mice injected with M202 (*Left*) and M207 (*Right*) tumors and scanned at the end point of the experiments with [^{18}F]FDG tracer injection. The upper right cube indicates mouse orientation: A, anterior; P, posterior, L, left; R, right. In addition, the left and right side of the mouse are indicated as *L* and *R* on the left and right sides of the animation.

Movie S7

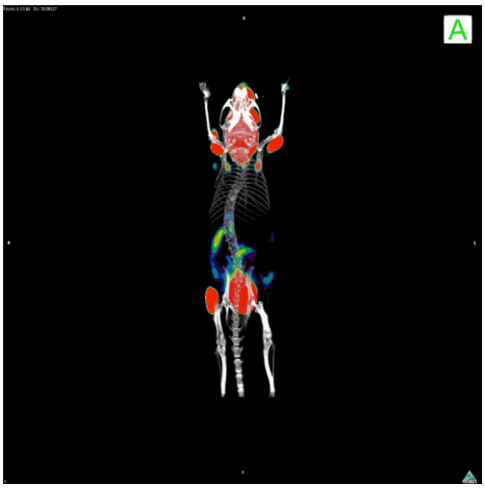

Movie S8. Reconstructed tridimensional PET CT scan. BLT mice injected with M202 (*Left*) and M207 (*Right*) tumors and scanned at the end point of the experiments with [^{18}F]FDG tracer injection. The upper right cube indicates mouse orientation: A, anterior; P, posterior, L, left; R, right. In addition, the left and right side of the mouse are indicated as *L* and *R* on the left and right sides of the animation.

Movie S8

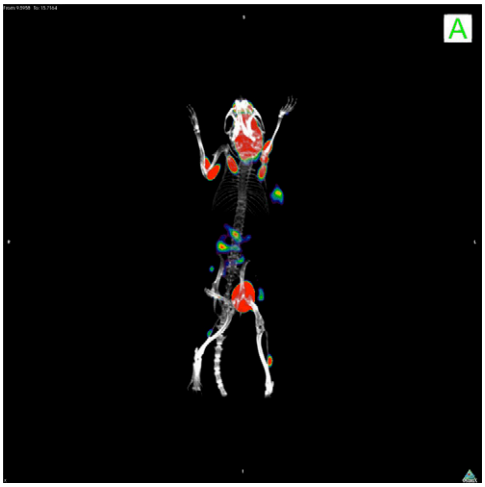

Movie S9. Reconstructed tridimensional PET CT scan. BLT mice injected with M202 (*Left*) and M207 (*Right*) tumors and scanned at the end point of the experiments with [^{18}F]FDG tracer injection. The upper right cube indicates mouse orientation: A, anterior; P, posterior, L, left; R, right. In addition, the left and right side of the mouse are indicated as *L* and *R* on the left and right sides of the animation.

Movie S9